2020

3D printing and characterization of hydroxypropyl methylcellulose and methylcellulose for biodegradable support structures

Prashant Ramkrishna Polampally
Iowa State University

3D printing and characterization of hydroxypropyl methylcellulose and methylcellulose for biodegradable support structures

by

Prashant Ramkrishna Polampally

A thesis submitted to the graduate faculty

in partial fulfillment of the requirements for the degree of

MASTER OF SCIENCE

Major: Industrial Engineering

Program of Study Committee:
Hantang Qin, Co-major Professor
Xiaolei Shi, Co-major Professor
Gül E. Kremer
Zheng Junxing

The student author, whose presentation of the scholarship herein was approved by the program of study committee, is solely responsible for the content of this thesis. The Graduate College will ensure this thesis is globally accessible and will not permit alterations after a degree is conferred.

Iowa State University

Ames, Iowa

2020

DEDICATION

This thesis is dedicated to my family and friends, who have raised me to be the person I am today. Thank you for the unconditional love, guidance and support that you have given me. Thank you for everything!

TABLE OF CONTENTS

Page

LIST OF FIGURES

Page

LIST OF TABLES

Page

NOMENCLATURE

FDM	fused deposition modeling
CAD	computer aided drawing
ME	material extrusion
MC	methylcellulose
HPMC	hydroxypropyl methylcellulose
SFF	shape fidelity factor
LVR	linear viscoelastic region
η	apparent viscosity (Pa·s)
G^*	complex modulus (Pa)
τ	shear stress (Pa)
τ_0	yield stress (Pa)
$\dot{\gamma}$	shear rate (s^{-1})
K	consistency index ($Pa \cdot s^n$)
n	flow behavior index

ACKNOWLEDGMENTS

I would like to thank my committee chair, Hantang Qin, and my committee members, Xiaolei Shi, Gul Kremer, and Zheng Junxing, for their guidance and support throughout the course of this research.

I also especially thank my colleagues Yiliang Cheng and Hunter Burnhart who helped me throughout my research work, without whom, this thesis would not have been possible.

Also, I would also like to thank my friends, colleagues, the department faculty and staff for making my time at Iowa State University an enjoyable experience.

ABSTRACT

Additive manufacturing processes based on fused deposition modeling (FDM) typically use thermoplastic materials like ABS, PLA, or nylon to fabricate parts layer-by-layer. In order to build a part successfully with complex features such as pores or holes or irregular shapes, the build part requires support structures to hold the deposited material and to prevent the collapse of the finished parts before solidification. The support material acts as a sacrificial layer that should be easily removed later by chemicals/enzymes or broken by mechanical force. The current support materials used with FDM technology have challenges of poor dissolvability in chemical solutions and difficulty to be removed from the finished part. Also, these support materials are usually petroleum-based which has a negative impact on the environment. The goal of the project is to identify a suitable biomaterial for support structures that will eliminate the challenges of poor dissolvability and toxic waste generated by the currently available support materials in the market. This paper is focused on extrusion-based 3D printing process of thermoset biopolymers to fabricate support structures using Material Extrusion (ME). In this study, three biodegradable cellulose derivatives (i.e. MC A4M, HPMC K4M, and HPMC E4M) used with different degrees of substitution of the hydroxyl group. We investigated the effect of concentrations (8, 10, and 12% w/v) of all three cellulose derivatives on the rheological properties for understanding their printability. The rheological analysis revealed that all hydrogels exhibit shear-thinning properties with relatively low yield stress. At the same concentration, the apparent viscosity of HPMC K4M tended to be higher than HPMC E4M, followed by MC A4M. The effects of printing parameters (extrusion rate, nozzle diameter, and printing speed) were optimized to obtain the desired three-dimensional structures. The samples of 12% MC A4M and 12% w/v HPMC K4M showed higher complex shear modulus than other

materials, which indicated higher rigidity and shape retention capacity of the printed parts. The ideal material for extrusion during printing and least deformation after printing was also observed for 12% MC A4M, which indicated a relationship between rheological properties and printability. The water dissolution of the MC and HPMC hydrogels allowed easy removal of the support structures from the build material. Biopolymers like MC and HPMC, when 3D printed as a support material via ME processes, help in moving closer towards sustainable manufacturing and a circular economy.

CHAPTER 1: INTRODUCTION

The on-demand economy is booming with 3D Printing as parts are customized when and where required. Three-dimensional (3D) printing is an additive manufacturing technique where successive layers of material printed on top of the previous layer based on digital model data inputs to fabricate the 3D object [1]. The advantages of 3D printing include the capability to form complex geometries, the possibility to integrate different materials through layer-by-layer modeling, speeding up product development cycles, and reducing prototyping cost. It offers a relative low-cost startup and supply chain to produce customized printed objects [2]. Fused deposition modeling (FDM) and material extrusion (ME) are the two most widely used 3D printing techniques. FDM technology developed in the early 1990's used polymers as the build material, e.g. Acrylonitrile Butadiene Styrene (ABS), Nylon, Polylactic Acid (PLA) [3].

1.1 Motivation

For constructing a three-dimensional part in FDM based 3D printing system requires support structures along with the primary structure for intricate and overhanging parts. The support structure is printed with a support material whereas primary structures are printed with primary or build material. Commercially available support materials in the market are high impact polystyrene (HIPS), Acrylic copolymers i.e. SR series from Stratasys, PVA etc. The support structure is a redundant part; hence it must be separated from the primary structure. The primary material should be handled carefully while removing the support material. These support materials are mostly petroleum plastics like the primary material in FDM based 3D printing. These plastics are non-renewable, non-biocompatible materials that are difficult to recycle.

Moreover, the support material is sometimes difficult to separate from the build material. The current support removal techniques leave behind toxic waste as it involves the use of chemical solvents. As of now, in FDM based 3D printing, there are no existing plant-based biomaterials that could be used as support material. Due to the drawbacks of the currently available support materials for 3D printing, there was a need for studying another support material. If plant-based cellulose derivatives used as a support material, it can act as a substitute for environmentally problematic plastics. This study focusses on assessing the printability and solubility of the plant-based cellulose derivatives in an environmentally friendly solvent.

1.2 Outline of the Thesis

This study focuses on finding an alternative suitable support material that could not only be 3D printed but also easily dissolved without the generation of toxic waste and hazardous fumes. Moreover, in the post-processing stage, the support material should be easily removable from the primary part by using an eco-friendly solvent. The modified cellulose ethers were mixed with water to form hydrogels with different compositions. The hydrogels with different compositions were further used for material characterization. To examine the printability of the materials, samples were subjected to rheological tests to assess their rheological properties. Based on the rheology results, the hydrogels were further investigated for dimensional accuracy. In the next stage, by varying the printer parameters with different concentrations of MC and HPMC, optimum parameters for accurate and stable 3D printing were explored. Further, to analyze the dissolvability of the hydrogels in water a solubility test was carried out. On solidification, the removal of plant-based support material from the build part will be faster and easier for FDM based 3D printing users.

CHAPTER 2: LITERATURE REVIEW

3D Printing is a process of prototyping where a part/product is built from its CAD (Computer-aided design) model. There are various 3D printing methods such as Digital light processing (DLP), Fused deposition modelling (FDM), Selective laser sintering (SLS), Selective laser melting (SLM), Electron beam melting (EBM), Laminated object manufacturing etc. This technology is extensively being used to make complex and customized products, which range from dental applications and intricate jewelry to parts for cars and aircraft. 3D printing facilitates faster development of ideas by creating prototypes with ease, thus saving time and money.

2.1 Fused Deposition Modeling

FDM is a rapid prototyping technique based on surface chemistry, thermal energy and layer manufacturing technology [4]. The part is initially designed in CAD and converted into an STL file (Stereolithography file format), to examine for defects like flip triangles, missing facets, overlapping facets, etc. and repaired if found faulty [5]. This defect free STL file is input into slicing software, which mathematically slices the model for build process. During the build process, filaments of thermoplastic, heated to its melting temperature are extruded layer by layer from a nozzle tip, which moves along the X-Y direction. The extruded material hardens upon solidification and bonds with the preceding layer. The base plate is maintained at a lower temperature to aid the cooling of the material when laid on it. Once the first layer of material laid, the platform lowers itself to allow the nozzle to lay the second layer onto it. Support layers are built along the way, fastened to the part either with a second weaker material or with perforated junction [4]. The main advantages of FDM include the

availability of a wide variety of thermoplastics, low maintenance cost, little need for supervision, and low-temperature operations [6].

2.2 Extrusion Deposition Printing

Extrusion based systems can be visualized as, like toothpaste extrusion from the tube; the material is forced through a nozzle when pressure is applied [7]. The difference between FDM and material extrusion(ME) system is the material used in the FDM system is in the filament form, whereas the material in the extrusion-based system is in the form of ink/gel.

In some cases, the FDM system requires support structures to build a part successfully [8]. The support structure acts as a sacrificial layer and enables the formation of cavities, hollow sections, and complex overhanging features for the build material. The support material is useful for other purposes as well, e.g., to minimize warping from the build material and to enable relative motion between two components. Support material can be printed with either similar deposition techniques as used in FDM for materials with high melting temperature, or with ME technique, which conducts direct extrusion of the prepared material from the paste extruder. For 3D printing of biopolymer and hydrocolloid materials as support material, the ME process is preferred due to the extrudability of such materials at ambient temperature. These biopolymer materials are typically thermoset instead of thermoplastic, which means they do not melt upon heating for extrusion like plastics, but form hydrogels with heat [9]. The hydrogels can be prepared and filled into paste extruder and then 3D printed as it is. The support material is subsequently removed or dissolved after the primary part is 3D printed [10].

The support material should be removable or be dissolvable without affecting the build material [11]. The present support materials used in the FDM system have challenges in terms of removability and sustainability. The use of pliers to remove the support structure

mechanically leaves some defective burrs on the surface of the primary part. Moreover, in such a process, some amount of support material is leftover in the cavities of support structures [12]. Another technique is heating the support material to a temperature above its melting point to remove the support material from the build material with minimum residue. In these cases, there will be an undesirable oily residue left on the printed three-dimensional part. Furthermore, the use of elevated temperatures to melt the support structures may affect the mechanical performance of the finished three-dimensional part resulting in part deformation or failure [13].

In FDM based ABS printing, polyvinyl alcohol (PVA) is commonly used as support material as it is a biodegradable material. After the primary part is printed and solidified, the support part fabricated with PVA is dissolved in a solution of isopropyl alcohol and potassium hydroxide to remove the support structures; however, it generates hazardous and toxic wastes [14]. Another commonly used support material is high impact polystyrene (HIPS), which can be dissolved by limonene for removal after 3D printing, but this process generates harmful toxic fumes [13]. The acrylic copolymer has been used as commercial support materials (e.g. SR series from Stratasys) to support FDM based 3D printing. However, they all have limitations during removal process. Manual mechanical removal only works for simple support structures, while bath decomposition generates hazardous bath solutions and chemical wastes that are not sustainable. Personal protective equipment, safe disposal methods according to local regulations and safe handling are required for post processing of acrylic polymer-based support materials.

US Patent No. 5, 503,785 disclosed that a release material can be deposited as a thin coating between the build material and the support material. The release material is a

hydrocarbon wax or a water-soluble wax, acrylates, polyethylene oxide, glycol-based polymers, polyvinyl pyrrolidone-based polymers, methyl vinyl ethers, maleic acid-based polymers, polyoxazoline-based polymers, Polyquaternium II or conventional mold release materials, such as fluorochemicals, silicones paraffins or polyethylene's. Depending on the type of release layer, it may also leave an undesirable oily residue on the completed three-dimensional part. Moreover, the release layer adds complexity to the three-dimensional printing of the parts [15].

US Patent. No. 6,070,107 proposes the use of poly(2 - ethyl - 2 - oxazolidine) as water-soluble support and mold material. However, on thermal decomposition of poly(2 - ethyl - 2 - oxazolidine) fumes are generated, specifically, nitrogen oxides and carbon oxide, as disclosed in its Material Safety Data Sheet [16].

Over the past few years, numerous research studies focusing on hydrocolloids and food materials have been done by adapting extrusion based FDM techniques. These materials are prepared before printing in the form of pastes and then extruded layer by layer without the need for melting the material [17]. This ME technique is suitable for materials that can be extruded at ambient temperature or slightly elevated temperature. For 3D printing, the materials are viscoelastic materials that are homogeneous and suitable for extrusion under certain conditions, as well as have excellent shape retention capacity. In general, the printability of the materials is related to viscoelastic properties represented by storage and loss modulus, viscosity and yield stress [18]. Liu et al. (2017) established the precision printing of extrusion-based materials by studying the importance of the rheological properties of the edible inks. For extrusion-based printers, it is crucial to understand the rheological properties of the material to be printed. The rheological parameters that may relate to the

extrudability during printing and deformation post-printing are viscosity, yield stress, and viscoelastic modulus [19]. The support material should exhibit suitable rheological properties for their compatibility with extrusion-based printers.

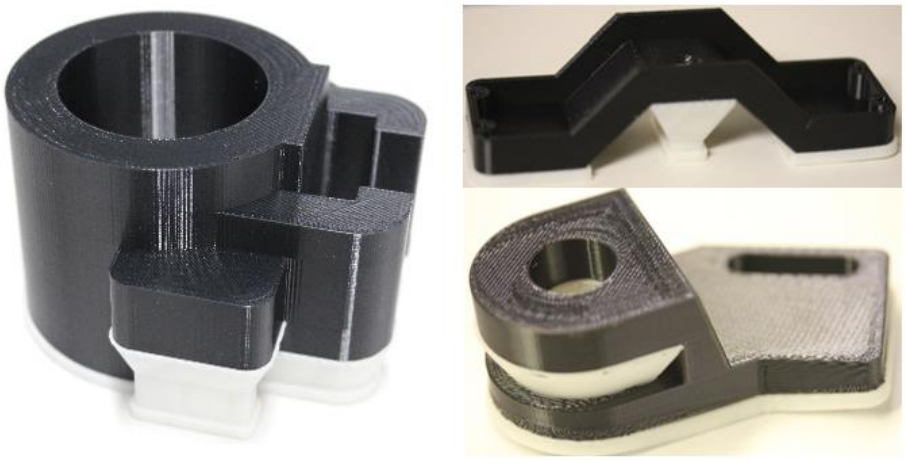

Figure 1 *Removal of support structures in FDM may damage printed parts and generate chemical hazards*

One group of the potential materials suitable for ME based 3D printing for support structures are cellulose derivatives. Cellulose is one of the most used natural polymers on the planet. Cellulose is hydrophilic, but as it has many hydroxyl groups that form hydrogen bonds, the intramolecular hydrogen bonding prevents itself from being dissolved in water. When the hydroxyl groups of cellulose structure are modified by methoxyl groups and hydroxypropyl groups, the derived semi-synthesized cellulose derivatives become water-soluble [20]. Methylcellulose (MC) is the simplest cellulose derivative and hydroxypropyl methylcellulose (HPMC) is a nonionic cellulose derivative material. The modified cellulose derivatives are widely used in the food industry and pharmacy field, such as a thickening agent in foods or drug matrix for controlled drug delivery, respectively [20, 21]. Cellulose ethers exhibit thermal gelation property, which is suitable for 3D printing of support

materials [22]. Such materials form gels upon heating and liquefy on cooling [23]. This thermal gelation property will make the hydrogels of cellulose ethers to dissolve easily in water. Typically, the major industrial source of cellulose is from plants such as refined cotton with an alkaline treatment. The cellulose derivatives such as MC and HPMC can be derived from cellulose by different processes such as oxidation, micronization, etherification and esterification [24].

CHAPTER 3. MATERIAL CHARACTERIZATION AND PRINTER DESIGN

3.1 Material Characterization

3.1.1 Materials

Cellulose is one of the most abundant polymers on Earth, mostly produced by plants. It is extensively used as a raw material in the paper industry in the production of paper and cardboard products [25]. Cellulose can be chemically modified to obtain cellulose derivatives to obtain desired properties. Cellulose ethers and Cellulose esters are two main groups of cellulose derivatives available in the market with different mechanical and pharmaceutical properties [26]. The three different materials of cellulose ether derivatives used in this study are MC A4M, HPMC E4M and HPMC K4M (J. Rettenmaier USA LP, Schoolcraft, MI). The degree of substitution (DS) of methoxyl groups for MC A4M is 27.5-31.5%. The DS of methoxyl groups is 28-30% for HPMC E4M and 19-24% for HPMC K4M, respectively. The DS of the hydroxypropyl group is 7-12% for E4M and 4-12% for K4M. All three materials have a viscosity of 3000-5600 mPa·s in 2% solution at 20°C.

The samples were prepared by mixing the powder into deionized water at 70°C to achieve different concentrations of 8%, 10%, 12% w/v. After cooling down to room temperature (25°C), all samples were centrifuged at 5000 rpm for 10 min to make homogenous hydrogels.

3.1.2 Rheological characterization

The study of rheological properties is critical to determine the effect of concentration on the printability and deformation of material during 3D printing. Firstly, the flow ramp test was conducted to determine the flow behavior and apparent viscosity of different materials at different concentrations. Then the yield stress and complex modulus were determined via the

oscillatory stress sweep test. The estimate of yield stress derived from the oscillatory sweep stress test was fitted into the Herschel-Bulkley model to obtain the values of flow consistency (*K*) and flow behavior index (*n*).

The samples prepared were subjected to rheological tests to assess their suitability for 3D printing. These tests were performed using a rotational rheometer (TA Instruments Discovery HR-2, USA) using parallel geometry plates (Peltier plate steel - 110870 40 mm plate) at a gap size of 1 mm under 25°C. Before the test, the excess material between the plates was trimmed. Both flow ramp test and oscillatory stress sweep test were conducted for each sample for 3 repetitions. Before the test, the samples were rest for 10 min between the parallels plates to achieve a steady state. To avoid evaporation, the sample and geometry plates were covered by a rheometer protect lid.

In the flow ramp test, the shear rate was set at 0.1-30 s^{-1} with linear test mode and the runtime was set at 30s. Apparent viscosity (η) was calculated by dividing shear stress to shear rate, with the unit of Pa·s. The flow curves were fitted to the Herschel-Bulkley model (Equation 1) as follows [27]:

$$\tau = \tau_0 + K\dot{\gamma}^n \quad (1)$$

where τ means shear stress (Pa), τ_0 is yield stress (Pa), $\dot{\gamma}$ is the shear rate (s^{-1}), *K* is the consistency index ($Pa \cdot s^2$), and *n* is the flow behavior index. As yield stress was determined by the oscillatory stress sweep test described below, *K* and *n* were calculated with the data derived from the flow ramp test according to Equation 1.

The oscillatory stress sweep test was performed at a frequency of 0.5 Hz. The sample was subjected to increasing sweep stress of 0.1-1000 Pa and the resulting strain was

recorded. Complex modulus (G^*) is calculated as the ratio of stress over the corresponding strain. When the sweep stress is below specific stress, there is a linear viscoelastic region (*LVR*) where the stress and strain are linearly proportional to each other and the G^* within the *LVR* is constant. The endpoint of the *LVR* corresponding to a specific stress value is considered as the critical stress [28]. For this study, the end of the *LVR* is marked by the first point where the G^* dropped by 10% of the G^* within the *LVR*, and the corresponding stress at this point is referred to as the estimate of yield stress.

3.2 3D Printer Setup

A customized extrusion-based printer is demonstrated in Fig. 2. A spur gear mechanism controlled by the motor drives the piston that allows the material in the syringe to extrude to fabricate part layer-by-layer on a plate. The base plate can cover X and Y directional movements, whereas the nozzle increments the height in Z-direction to print on top of each layer. The sliced part/design of the final product is fed into the 3D printer as G-Codes.

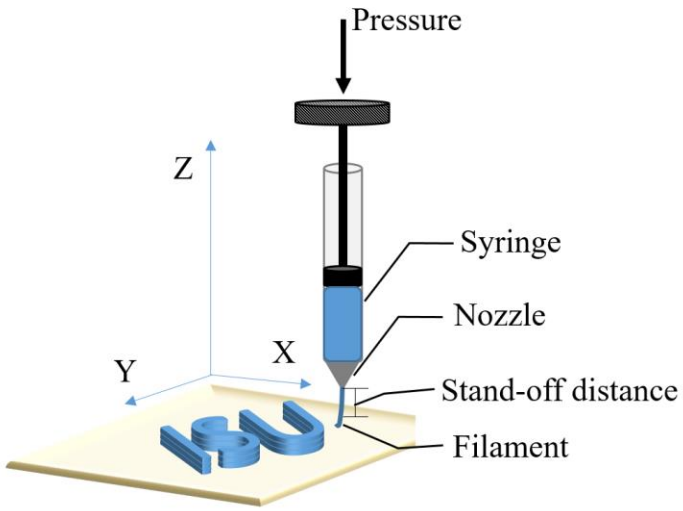

Figure 2 *Schematic diagram of the extrusion-based printer setup*

For printability study, the concentration of the cellulose derivatives in the hydrogels was optimized based on dimensional accuracy. An extrusion multiplier of 0.125 and a nozzle diameter of 0.508 mm were used for all the concentration optimization experiments. Three lines were printed with a spacing of 20 mm. The morphology of the filaments was observed using a digital camera (Canon EOS Digital Rebel T3i). The filament width was measured and calculated by digital image processing algorithms. For higher dimensional accuracy and a high-density support structure, the slumping of deposited layers was assessed in terms of shape fidelity factor [29]. Shape fidelity factor (SFF) is the ratio of any side of the printed area to the CAD model area. Shape stability was evaluated by using an image analyzer to calculate the area of the printed geometry. To assess the shape stability, three cubes with 12% concentration of HPMC K4M, HPMC E4M and MC A4M were printed with 1 mm x 1 mm x 1 mm dimensions. The effect of nozzle diameter on the printed filament was analyzed. For each type of hydrogel composition, three lines having a 50 mm length is deposited with six different nozzle diameters ranging from 0.437 mm to 1 mm.

CHAPTER 4. RESULTS AND DISCUSSION

This section consisted of the analysis of the rheological experiments and discussion about the fluid behavior of the cellulose-derived hydrogels when it went under extrusion in a printer. The oscillatory sweep test was discussed for calculating the yield stress, which is a key factor for initiating any extrusion process. After validating whether the materials could be printed in 3D or not, the next step was printability analysis. The optimal concentration of the material was identified by performing dimensional analysis. The optimal concentration was chosen and further subjected to shape fidelity test. Then the suitable material that passed shape fidelity test was subjected to a solubility test. Finally, different geometries were 3D printed with optimal printing parameters and concentrations to showcase the printability.

4.1 Flow Ramp Test

The flow curves (Fig. 3) of MC A4M, HPMC K4M, HPMC E4M at 8%, 10%, and 12% w/v concentrations indicated shear-thinning behavior for all samples. A plot of the apparent viscosity as a function of shear rate is shown in Fig. 4. As the concentration increased, there was an increase in shear stress and apparent viscosity. The apparent viscosity significantly decreased as the increase in shear rate. This decrease in viscosity with increase in shear rate can be explained as the macromolecular network amongst the molecules were deformed or reorganized during shearing [21]. The highest apparent viscosity was observed for 12% HPMC K4M, followed by 12% MC A4M and then 12% HPMC E4M. The standard deviations for 12% MC A4M were relatively significant than other materials. The 12% MC exhibits more solid-like behavior as compared to 12% HPMC K4M and 12% HPMC E4M. Upon shearing, it formed thin films between parallel plates, making it not suitable to be tested by flow ramp test under the conditions provided.

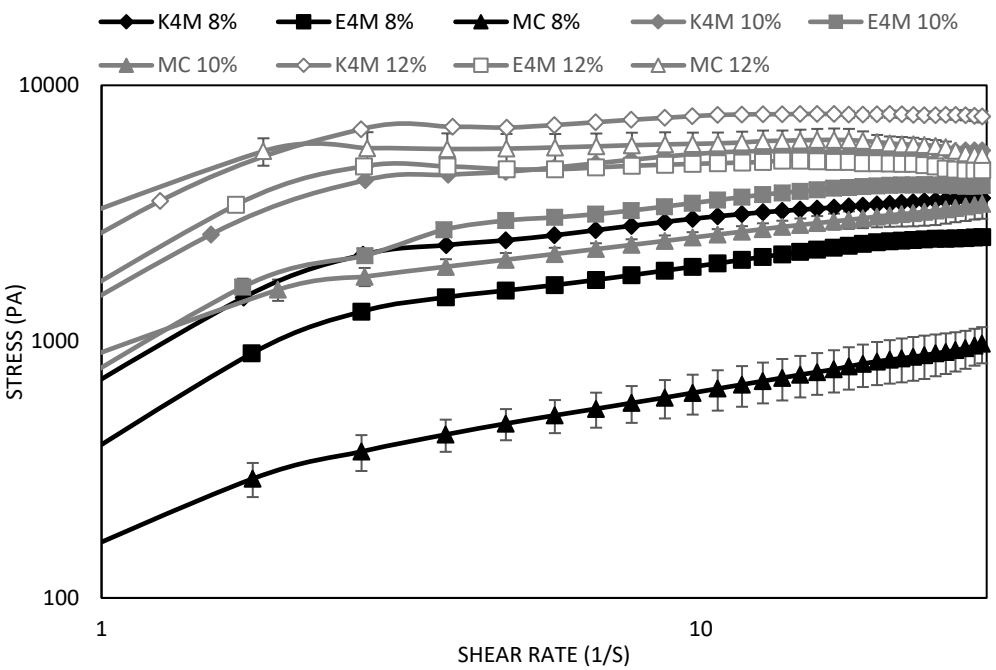

Figure 3 *Flow curves of hydrogels of HPMC K4M, HPMC E4M, and MC A4M with 8%, 10%, 12% w/v at 25°C on a log scale*

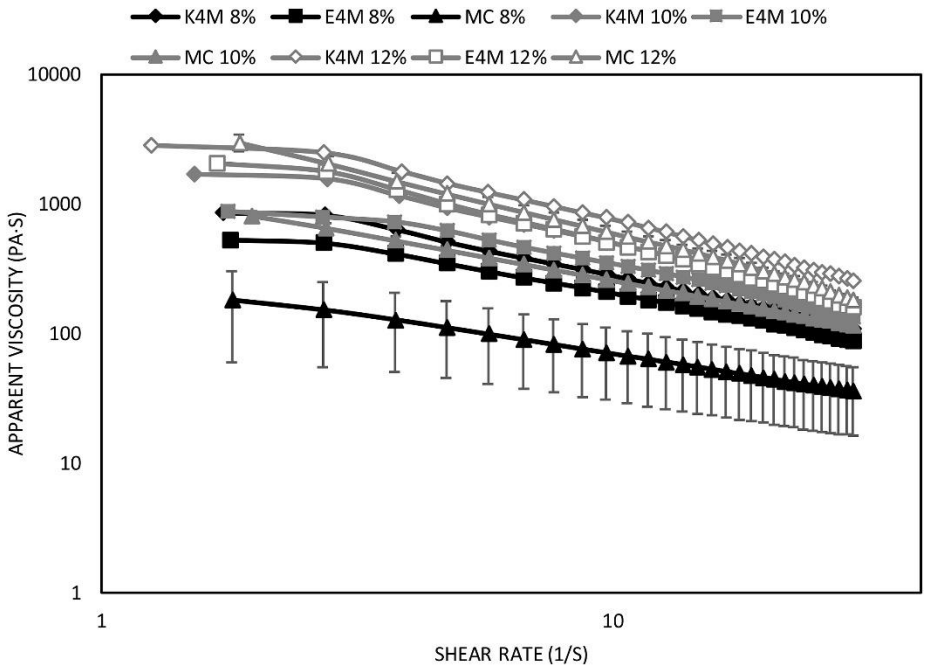

Figure 4 *Apparent viscosity versus shear rate profiles of HPMC K4M, HPMC E4M, and MC A4M with 8%, 10%, 12% w/v at 25°C.*

4.2 Oscillatory Stress Sweep Test

The oscillatory stress sweep test is to determine the critical stress, i.e. the amount of yield stress, using the stress value at the endpoint of *LVR*. Furthermore, the complex modulus is a measure of the rigidity of the sample [28]. Fig. 5 shows the complex modulus as a function of oscillation stress for different materials at different concentrations. From the graph, it shows that the critical stress increased with the increase of concentration for each material. The highest critical stress was observed for 12% MC A4M, while the lowest critical stress was 8% MC A4M, which means the material of MC A4M can reach a wide range of the critical stress values by adjusting its concentration. Before the stress reached the critical stress, the hydrogels remained three-dimensional rigid networks due to intramolecular forces, but upon the yield point, the networks between the particles were fractured and the sample started to flow [29]. For complex modulus, the highest value was also observed for 12% MC A4M (24235.26 Pa), followed by 10% MC A4M (18175.39 Pa) and 12% HPMC K4M (12906.43 Pa). As 12% MC showed both the highest yield stress and G^*, it indicated that 12% MC is the most rigid sample and it takes the highest stress to initiate flow, thus it may be the hardest to be extruded during 3D printing and it may undergo the least deformation after 3D printing. The relationship between rheological properties and extrudability/deformation of 3D printing can be further determined by investigating the printability and shape fidelity for different samples, as described below.

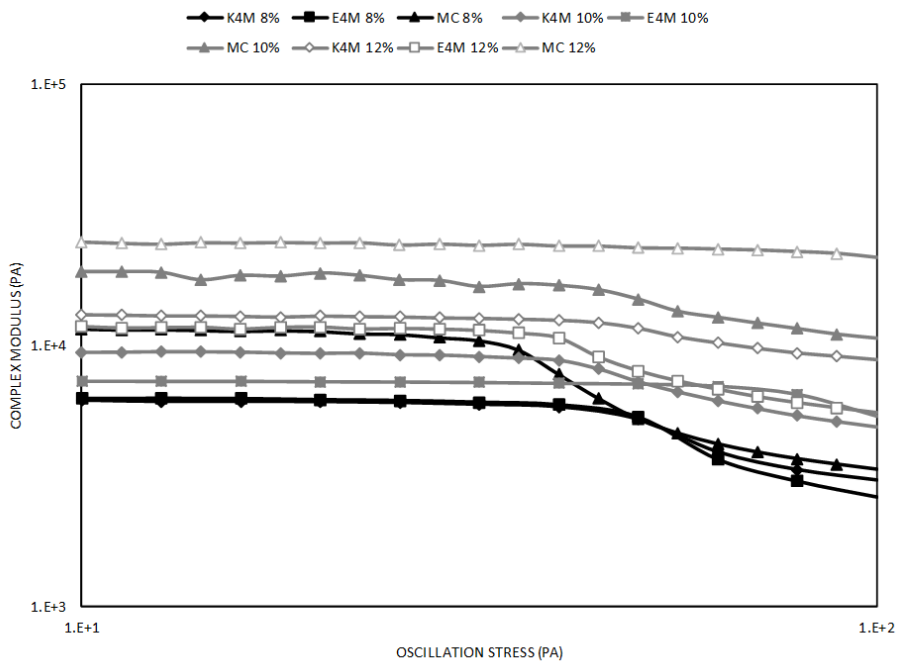

Figure 5 *Oscillation stress versus complex modulus profiles of HPMC K4M, HPMC E4M, and MC A4M with 8%, 10%, 12% w/v at 25°C.*

Table 1 *Herschel-Bulkley model parameters for the flow curves of HPMC K4M, HPMC E4M, MC A4M samples*

Material	**Concentration %**	**Estimated τ_0 (Pa)**	***K* (Pa·s^n)**	***n***
HPMC K4M	8	37.09	1910.73	0.16
	10	41.81	4073.80	0.07
	12	45.10	6481.87	0.05
HPMC E4M	8	43.26	1060.47	0.27
	10	65.56	2195.33	0.18
	12	39.99	3836.19	0.11
MC A4M	8	29.46	592.38	0.34
	10	43.05	1318.56	0.28
	12	95.69	5222.76	0.05

Once yield stress was estimated via oscillation test, the value of flow consistency (*K*) and flow behavior index (*n*) can be derived from the Herschel-Bulkley model based on flow curves (Fig. 3). Table 1 presented the flow parameters of all samples. The yield stress, *K*, and *n* are critically determining the material rheological properties and printability performance. The flow behavior exponent less than 1 ($n<1$) indicates that all these materials are shear-thinning [30] (Table 1).

Based on the data, the value of yield stress and *K* both increased as the concentration increased. The value of n decreased as the concentration increased. In general, HPMC E4M showed the highest yield stress among the three materials at the same concentration. Besides, the *n* value of HPMC K4M samples is significantly smaller than the other samples at the same concentration. In this case, HPMC K4M is the most shear stable material compared with HPMC E4M and MC A4M [22]. The lower *n* also means the material has more pronounced non-Newtonian flow behavior when *n* less than one. Higher *K* value indicates the material becomes more pseudoplastic and more viscous [21]. As seen in Table 1, the lower value of *n* indicated that HPMC K4M hydrogels showed more obvious non-Newtonian behavior compared with the other two materials at the same concentration. For flow consistency, the comparison of *K* demonstrated that HPMC K4M hydrogels are the most pseudoplastic and more viscous samples and MC A4M hydrogels are the less pseudoplastic and less viscous samples with the same concentration. When the concentration increased for each material content, the value of *K* increased, and *n* decreased for all these three materials. These results indicated that the concentration variation of these three materials significantly influences the flow behavior of the hydrogels, which may also have an influence on their extrusion during 3D printing and deformation after 3D printing.

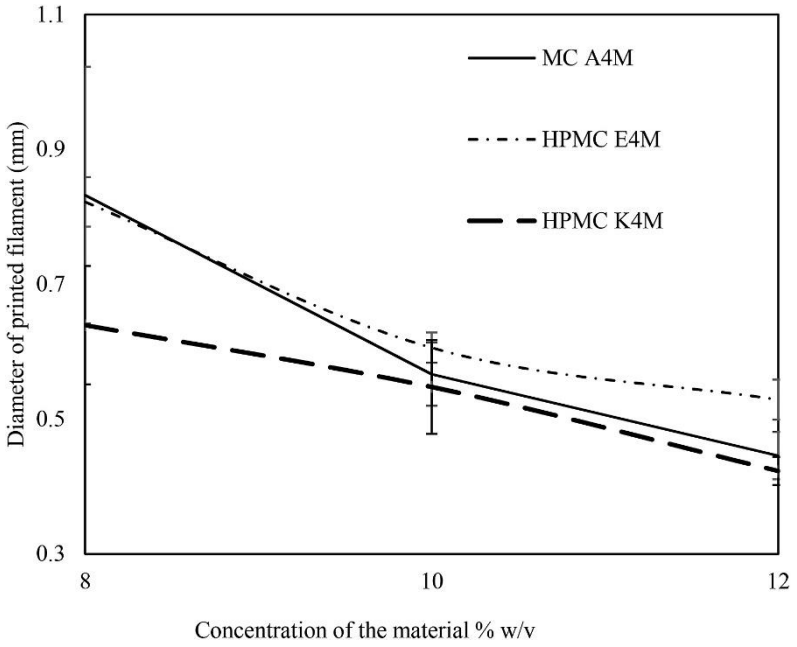

Figure 6 *Diameter of printed filament versus concentration of the material in the hydrogels*

4.3 3D Printing

4.3.1 Optimization of concentration

An ideal hydrogel should have a sufficiently high gel strength, proper viscosity and be capable of fusing with the earlier printed layers, as well as retain the print shape [31]. Standardized methods to evaluate the printability of hydrogel is not yet established. Optimization of the concentration is significant to find the ideal condition for printing. The optimal concentration was found by printing three lines of each concentration keeping all the other printer parameters constant. The nozzle diameter chosen was 0.437 mm, printing speed of 5 mm/s and extrusion multiplier of 0.125. The three lines printed were given to the printer software in the form of a G-code. The diameter of the printed filament was measured using Image analysis software. It was observed that with an increase in the concentration of the material the diameter of the filament was decreasing, as shown in Fig. 6. This was due to increase in apparent viscosity with an increase in the concentration of the material. The

cellulose derivatives with lower concentration when printed on a surface will spread out on the surface due to the low viscosity and high flow behavior index value ‘n.’ The 12% w/v of all three materials had the filament diameter close to nominal nozzle diameter. The 12% w/v of all the three materials were chosen for further printability analysis as it had the least deviation from the mean.

4.3.2 Shape fidelity

The shape fidelity test quantitatively evaluates the physical deformation of the printed geometries. Higher the shape fidelity factor, lower the ability of the material to stack up in layers i.e. the printed part deforms after depositing few layers [32, 33]. This test will provide meaningful insights into the shape of the printed part after the printing process. The image of the top view of the printed cubes with 12% w/v for all three cellulose derivatives is as shown in Fig. 7. The printed area is calculated using SketchandCalc Area calculator. The scale was defined by specifying the number of pixels required for 1 mm length. The top view of the image is imported into the software. The software will detect the boundary of the image and define the number of pixels inside the boundary. The printed area is calculated based on the number of pixels and the length of each pixel. The printed area is larger for HPMC E4M compared to HPMC K4M and MC A4M. Since, the HPMC E4M deforms while stacking up in layers. The shape fidelity factor for each cellulose derivative is given in Table 2. This deformation is because of the lower value of the complex shear modulus, as shown in Fig. 5. Shape fidelity of geometry upon deposition is largely influenced by complex shear modulus (G^*). 12% w/v of MC A4M has higher complex shear modulus than 12% w/v of HPMC E4M; thus, MC A4M has higher shape retention capacity and lower shape fidelity factor. The 12% HPMC E4M has shape fidelity factor of 1.39, indicating a significant deformation of the layers. Hence the 12 % HPMC E4M is not suitable for printing.

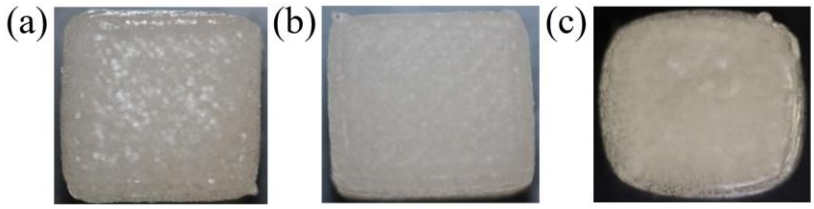

Figure 7 *Top view of the cube for 12% w/v concentrations for (a) HPMC K4M (b) MC A4M and (c) HPMC E4M*

Table 2 *Shape fidelity factor based on CAD and printed shapes*

Material (12% w/v)	**CAD Area (mm^2)**	**Printed area (mm^2)**	**SFF**
HPMC K4M	100	122	1.22
HPMC E4M	100	139	1.39
MC A4M	100	110	1.1

4.3.3 Effect of nozzle diameter on printability

The printability of the hydrogel is not only affected by the rheological parameters and its concentration but also affected by printing parameters such as extrusion multiplier, feed rate, and nozzle diameter. In an extrusion-based 3D printer, the printer parameters are optimized at which continuous filaments with a uniform diameter could be deposited. The extrusion multiplier for the printer is set at 0.125 and feed rate of 5 mm/s. Six different nozzle diameter ranging from 0.437 mm to 1.0 mm was used to print the three lines. Fig. 4.6 Shows the relationships between filament diameter and nozzle diameter. For both the materials 12% w/v of MC A4M and HPMC K4M, the nozzle diameter had the same effect. The diameter of printed filament decreases with the reduction in the size of the nozzle diameter. The diameter of the printed filament is proportional to the resolution of the part being printed. Smaller the nozzle diameter better is the resolution of the printed geometry. Hence, the nozzle diameter of 0.437 mm was chosen to print the 3D objects.

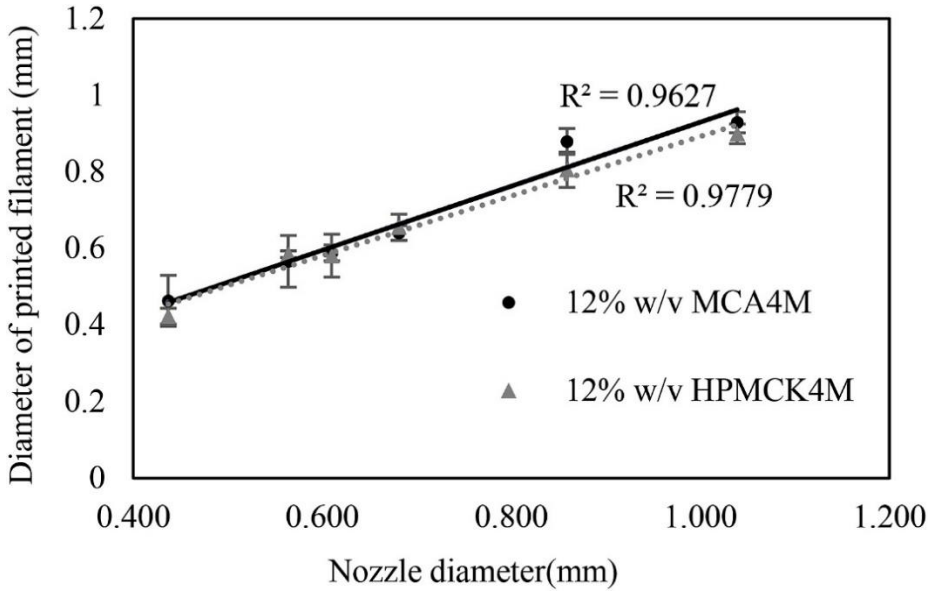

Figure 8 *Diameter of printed filament versus nozzle diameter for 12% w/v MC A4M and HPMC K4M*

4.3.4 Solubility test

The solubility test assesses the dissolvability of the printed cellulose derivatives in water. It is essential to perform this test to find how easily the support material is soluble or removable from the primary material. A visual inspection of the solubility test revealed the dissolvability behavior of the cellulose derivatives. Post-processing of the support structures by dissolving it in a water bath at 20℃ was analyzed. Two cubes were printed for 12% w/v HPMC K4M and 12% w/v MC A4M with a nozzle diameter of 0.437 mm and a feed rate of 5 mm/s. The cubes were then immersed in a water bath at 20℃ for 8 hours. Images were captured at two-hour intervals to observe the phase change, as shown in Fig. 9. At the end of the solubility test, both 12% w/v HPMC K4M and 12% w/v MC A4M became soft and dissolved partially into the water. This dissolution of cellulose derivatives is due to their thermal gelation property. As a result, these cellulose derivatives can be extensively used for building support structures in the highly viscous state at ambient temperature and dissolve

the support structure after printing by immersing in a cold bath at 20℃. This thermal gelation property enables easy removal of the support structures with non-toxic wastes from the build materials.

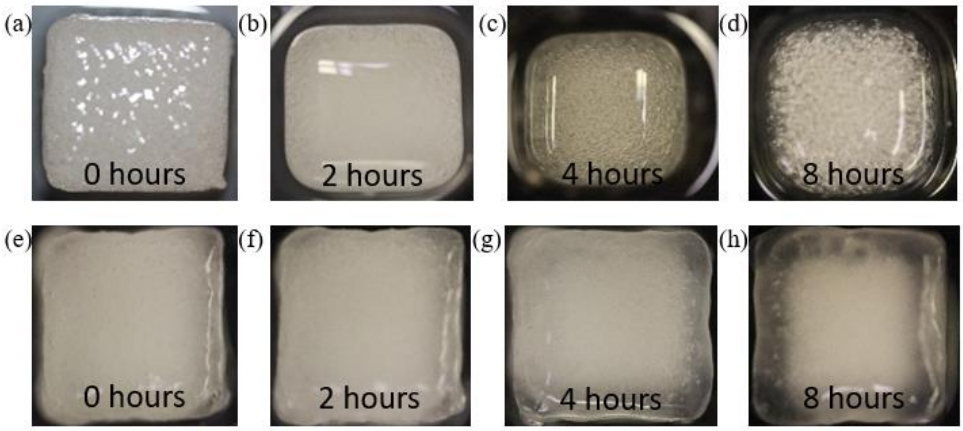

Figure 9 *(a-d) 12% w/v HPMC K4M and (e-h) 12% w/v MC A4M dissolved in water for 8 hours with 2-hour interval*

4.4 3D Printed Parts

Different geometries, as shown in Fig. 10 were 3D printed to validate the obtained rheology and printability results. Hydrogels of 12% w/v HPMC K4M and 12% w/v MC A4M were used to print the geometries at a printing speed of 5 mm/s and a nozzle diameter of 0.437 mm. All the printed geometries were at the macro level. The pyramid had a base of 20 mm (Fig. 10. (a)), a cube with 10 mm side (Fig. 10. (b)), logo (Fig. 10. (c)) and ISU letters (Fig. 10. (d)) had 40 mm. The honeycomb pattern with each hexagon of 8 mm side was printed (Fig. 10. (e)).

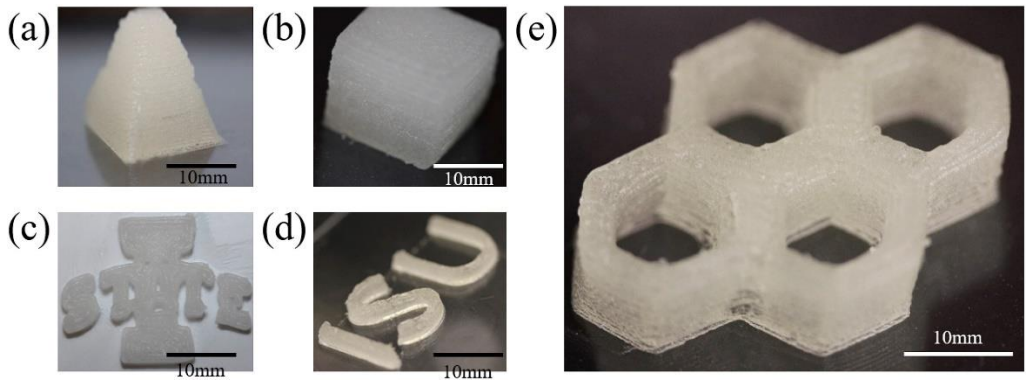

Figure 10 *(a) Pyramid with 12% HPMC K4M, (c) Iowa State University logo 12% HPMC K4M, (d) ISU letters 12% HPMC K4M and (e) Honeycomb pattern printed with 12% HPMC K4M; (b) Cube printed with 12% MC A4M*

CHAPTER 5. CONCLUSION AND FUTURE SCOPE

Three different types of cellulose derivatives were analyzed for their possible use as support materials in 3D printing. An effect of the extrusion process on the cellulose hydrogels was observed by using the rheology tests to understand their viscosity. Based on the data obtained from the flow ramp tests, it was validated that these cellulose-based hydrogels can be printed as they show shear thinning behavior. The yield stress was determined with oscillatory sweep test, the shear-thinning property was characterized by a viscosity versus shear rate graph and the obtained curve was fitted via the Herschel Bulkley model to understand about their consistency index (K) and flow behavior index (n).

The optimal concentration of the cellulose derivatives was determined based on dimensional analysis and it was found to be 12% w/v concentration for all the three materials. Further, the retention capacity was assessed by shape fidelity factor. Based on SFF, it was discovered that 12% w/v of HPMC E4M is not suitable for printing due to the lower complex shear modulus. The width of the printed lines can be varied by changing the parameters of the printer like print speed, extrusion rate, and nozzle diameter. The optimum printing parameters will help in printing support structures with controlled dimensions and complex geometries. Cellulose-based hydrogels can be used for printing support structures as they liquefy on cooling and they easily dissolve in water due to their thermal gelation property. The hydrogels of 12% w/v of HPMC K4M and MC A4M hydrogels were successfully 3D printed using a material extrusion-based printer. These materials, when used as the support structure in 3D printing, will eliminate the toxic waste generated, which were generated by conventional dissolution methods. Cellulose-based derivates as support materials will be an alternative that will reduce the negative impact on the environment.

These biodegradable polymers will not only help in reducing waste but also creating a footprint towards a sustainable environment.

The future scope of the project involves the simultaneous printing of ABS polymer with cellulose derivatives as support structures. This project will include developing a dual extruder printer for simultaneous printing and evaluating the compatibility of ABS (primary material) - cellulose derivative (support material) interface. The ultimate aim will be to create a sustainable FDM based 3D printing from a niche market to mainstream. Apart from using cellulose-based materials as support materials, they can be used in a wide range of applications from medicine to tissue engineering [34, 35, 36].

This thesis work is the was presented at 47th North American Manufacturing Research Conference 2019 and successfully published in 2019 “Polymer” Journal with the title “3D printing and characterization of hydroxypropyl methylcellulose and methylcellulose for biodegradable support structures.” The journal publication is available on this link: https://doi.org/10.1016/j.polymer.2019.04.013

REFERENCES

[1] Tenhunen, T-M., Varis, P., Kammiovirta, K., Puolakka, A., Setälä, H., Harlin, A., Orelma, H. 3D-printing of cellulosic materials: Properties and suitability on cellulosic fabrics. 253rd ACS National Meeting. San Francisco, United States; 2017.

[2] Van Wijk, A. 3D Printing with Biomaterials - Towards a Sustainable and Circular Economy, IOS Press; 2015.

[3] Stansbury, J. W., & Idacavage, M. J. 3D printing with polymers: Challenges among expanding options and opportunities. Dental Materials; 2016, 32(1), p. 54-64.

[4] Christiyan, K. J., Chandrasekhar, U., & Venkateswarlu, K. A study on the influence of process parameters on the Mechanical Properties of 3D printed ABS composite. In IOP Conference Series: Materials Science and Engineering. (2016) (Vol. 114, No. 1, p. 012109). IOP Publishing.

[5] Subramanian S. M., Monica M. S., Handbook of Sustainability in Additive Manufacturing, Volume 2, Springer; 2016.

[6] Zhang, Y., & Chou, K. A parametric study of part distortions in fused deposition modelling using 3-dimensional finite element analysis. Proceedings of the Institution of Mechanical Engineers, Part B: Journal of Engineering Manufacture; 2008, 222(8), 959-968.

[7] Gibson, I., Rosen, D. W., & Stucker, B. Extrusion-based systems. In Additive Manufacturing Technologies; 2010, (pp. 160-186). Springer, Boston, MA.

[8] Priedeman Jr., W. R and A.L.Brosch. Soluble Material; and Process for Three-Dimensional Modeling. United States Patent No. US 6790403; 2004. Washington, DC: U.S. Patent and Trademark Office.

[9] Kapur PC, Scales PJ, Boger D V, Healy TW. Yield Stress of Suspensions. Loaded with Size Distributed Particles. AIChE Journal; 1997, 43, p. 1171-1179.

[10] Collins, D.C., J.A.Nielsen, I. Faar, and C. OriaKhi. Use of support material in Solid Free form Fabrication Systems. United States Patent No. US 0072113; 2005. Washington, DC: U.S. Patent and Trademark Office.

[11] Gebhardt, A. Rapid prototyping / Andreas Gebhardt. (1st ed.). Hanser Gardener Publications, Munich: Cincinnati: Hanser; 2003.

[12] Park, S. J., Lee, J. E., Park, J. H., Lee, N. K., Lyu, M., Park, K., … Park, S. Enhanced Solubility of the Support in an FDM-Based 3D Printed Structure Using Hydrogen Peroxide under Ultrasonication. Advances in Materials Science and Engineering; 2018.

[13] Bayer, R., Wagner, A., Pyzik, A. J., Allen S. Support materials for 3D printing. United States Patent No. 20180147785; 2018. Washington, DC: U.S. Patent and Trademark Office.

[14] Park, S. J., Lee, J. E., Park, J. H., Lee, N. K., Lyu, M. Y., Park, K., ... & Park, S. H. Enhanced Solubility of the Support in an FDM-Based 3D Printed Structure Using Hydrogen Peroxide under Ultrasonication. Advances in Materials Science and Engineering; 2018.

[15] Scott Crump, Wayzata; James W. Comb, St. Louis Park; William R. Priedeman, Jr., Wayzata; Robert L. Zinniel. Process of support removal for fused deposition modeling. U.S. Patent No. 5,503,785; 1996. Washington, DC: U.S. Patent and Trademark Office.

[16] John Lang Lombardi; Dragan Popovich; Gregory John Artz. Water soluble rapid prototyping support and mold material. U.S. Patent No. 6,070,107; 2000. Washington, DC: U.S. Patent and Trademark Office.

[17] Wegrzyn, T. F., Golding, M., & Archer, R. H. Food Layered Manufacture: A new process for constructing solid foods. Trends in Food Science & Technology; 2012, 27(2), 66-72.

[18] Liu, Z., Zhang, M., Bhandari, B., & Yang, C. Impact of rheological properties of mashed potatoes on 3D printing. Journal of Food Engineering; 2018, 220, p. 76-82.

[19] Liu, Z., Zhang, M., Bhandari, B., & Wang, Y. 3D printing: Printing precision and application in food sector. Trends in Food Science & Technology; 2017, 69, p. 83-94.

[20] Edelby, Y., Balaghi, S., & Senge, B. Flow and sol-gel behavior of two types of methylcellulose at various concentrations. AIP Conference Proceedings; 2014, 1593, p. 750-754.

[21] Ding, C., Zhang, M., & Li, G. Rheological properties of collagen/hydroxypropyl methylcellulose (COL/HPMC) blended solutions. Journal of Applied Polymer Science; 2014, 131(7), p. 1-10.

[22] Sarkar, N. Thermal gelation properties of methyl and hydroxypropyl methylcellulose. Journal of applied polymer science; 1979, 24(4), p. 1073-1087.

[23] Levy, A. Reverse thermal gels and the use thereof for rapid prototyping. United States Patent No. 6863859B2; 2005. Washington, DC: U.S. Patent and Trademark Office.

[24] Kulkarni, P., & Dixit, M. Sources of cellulose and their applications- A review. International Journal of Drug Formulation and Research; 2015, 2, p. 19-38.

[25] Liu, Z., Zhang, M., Bhandari, B., & Yang, C. Impact of rheological properties of mashed potatoes on 3D printing. Journal of Food Engineering; 2018, 220, p. 76-82.

[26] De Graef, V., Depypere, F., Minnaert, M., & Dewettinck, K. Chocolate yield stress as measured by oscillatory rheology. Food Research International; 2011, 44(9), p. 2660-2665.

[27] Klemm, D., Philipp, B., Heinze, T., Heinze, U., Wagenknecht, W. Comprehensive Cellulose Chemistry, Volume 1, Fundamentals and Analytical Methods, Wiley-VCH, Weinheim, 1998.

[28] Shokri, J., & Adibkia, K. Application of cellulose and cellulose derivatives in pharmaceutical industries. Cellulose-medical, pharmaceutical and electronic applications; 2013.

[29] Kapur PC, Scales PJ, Boger D V, Healy TW. Yield Stress of Suspensions Loaded with Size Distributed Particles. Particle Technology and Fluidization; 1997, 43, p. 1171-1179.

[30] Hamilton, C. A., Alici, G., & in het Panhuis, M. 3D printing Vegemite and Marmite: Redefining "breadboards." Journal of Food Engineering; 2018, 220, p. 83–88.

[31] Yang, F., Zhang, M., Bhandari, B., & Liu, Y. Investigation on lemon juice gel as food material for 3D printing and optimization of printing parameters. Food Science and Technology; 2018, 87, p. 67-76.

[32] Ribeiro, A., Blokzijl, M. M., Levato, R., Visser, C. W., Castilho, M., Hennink, W. E., Vermonden, T., & Malda, J. Assessing bioink shape fidelity to aid material development in 3D bioprinting. Biofabrication; 2017, 10(1), p. 9.

[33] Panda, B., & Tan, M. J. Experimental study on mix proportion and fresh properties of fly ash based geopolymer for 3D concrete printing. Ceramics International; 2018, 44(9), p. 10258-10265.

[34] Paggi, R. A., Salmoria, G. V., Ghizoni, G. B., de Medeiros Back, H., & de Mello Gindri, I. (2019). Structure and mechanical properties of 3D-printed cellulose tablets by fused deposition modeling. The International Journal of Advanced Manufacturing Technology, 100(9-12), 2767-2774.

[35] Jovic, T. H., Kungwengwe, G., Mills, A., & Whitaker, I. S. Plant-Derived Biomaterials: A Review of 3D Bioprinting and Biomedical Applications. Frontiers in Mechanical Engineering; 2019, 5, 19.

[36] Chia, H. N., & Wu, B. M. Recent advances in 3D printing of biomaterials. Journal of biological engineering; 2015, 9.